Cellular/Molecular

p53-Dependent Transcriptional Control of Cellular Prion by Presenilins

Bruno Vincent,[1,2] Claire Sunyach,[1,2] Hans-Dieter Orzechowski,[3] Peter St George-Hyslop,[4,5] and Frédéric Checler[1,2]

[1]Institut de Pharmacologie Moléculaire et Cellulaire and [2]Institut de Neuro-Médecine Moléculaire, Unité Mixte de Recherche 6097 Centre National de la Recherche Scientifique/Université de Nice-Sophia-Antipolis, Equipe labellisée Fondation pour la Recherche Médicale, 06560 Valbonne, France, [3]Institute of Clinical Pharmacology and Toxicology, Charité-Universitaetsmedizin Berlin, 10117 Berlin, Germany, [4]Centre for Research in Neurodegenerative Diseases, Department of Medicine, University of Toronto and University Health Network Toronto Western Hospital Research Institute, Toronto, Ontario M5S 3H2, Canada, and [5]Cambridge Institute of Medical Research, University of Cambridge, Cambridge CB2 OXY, United Kingdom

The presenilin-dependent γ-secretase processing of the β-amyloid precursor protein (βAPP) conditions the length of the amyloid β peptides (Aβ) that accumulate in the senile plaques of Alzheimer's disease-affected brains. This, together with an additional presenilin-mediated ε-secretase cleavage, generates intracellular βAPP-derived fragments named amyloid intracellular domains (AICDs) that regulate the transcription of several genes. We establish that presenilins control the transcription of cellular prion protein (PrP^c) by a γ-secretase inhibitor-sensitive and AICD-mediated process. We demonstrate that AICD-dependent control of PrP^c involves the tumor suppressor p53. Thus, p53-deficiency abolishes the AICD-mediated control of PrP^c transcription. Furthermore, we show that p53 directly binds to the PrP^c promoter and increases its transactivation. Overall, our study unravels a transcriptional regulation of PrP^c by the oncogene p53 that is directly driven by presenilin-dependent formation of AICD. Furthermore, it adds support to previous reports linking secretase activities involved in βAPP metabolism to the physiology of PrP^c.

Introduction

Transmissible spongiform encephalopathies (TSE) result from the unconventional conversion of the normal cellular prion protein (PrP^c) into its pathogenic, protease-resistant scrapie isoform $PrP^{s.c.}$ (Aguzzi and Polymenidou, 2004). The propagation mechanism apparently does not require any nucleic acid as was proposed in the "protein only" theory (Prusiner, 1998). Tremendous efforts have been devoted to understand the mechanisms by which PrP^c converts into $PrP^{s.c.}$ Although the precise process remains to be established, it appears clearly that "prion infection" requires the crucial presence of endogenous PrP^c, since PrP^c-deficient mice are fully resistant to infection and toxicity after inoculation with pathogenic scrapie-enriched material (Büeler et al., 1993; Brandner et al., 1996). However, since prion diseases are extremely rare with no more than one case per million of individuals in human beings, it is important to understand the physiological role and regulation of PrP^c.

PrP^c was reported to participate in lymphocyte activation (Cashman et al., 1990), cellular adhesion processes (Rieger et al., 1997; Gauczynski et al., 2001; Mangé et al., 2002), neurite growth (Santuccione et al., 2005), synaptogenesis (Kanaani et al., 2005), cellular signaling (Mouillet-Richard et al., 2000), and cell viability (for review, see Linden et al., 2008). Concerning transcriptional regulation of PrP^c, it has been reported that PrP^c mRNA levels could be increased either under stress conditions such as ischemia and hypoglycemia, or by some growth factors (Linden et al., 2008). However, little is known about the molecular pathways underlying these regulatory events. The functional characterization of the human prion promoter (Funke-Kaiser et al., 2001) identified two regulatory regions where sequence analysis revealed consensus sequences for AP-1, Sp1, and Sp2 factors (Mahal et al., 2001; Bellingham et al., 2009). Our *in silico* analysis of the human PRioN protein (*PRNP*) gene promoter also revealed a motif partly matching the binding sequence targeted by the oncogene p53. We have examined the ability of p53 to modulate PrP^c promoter transactivation and mRNA expression and we show that p53 acts as a transcriptional activator of PrP^c by binding directly to the suspected promoter sequence. Furthermore, we previously established that the β-amyloid precursor protein (βAPP-intracellular domain amyloid intracellular domain (AICD) generated after presenilin-dependent γ-secretase-mediated cleavage of βAPP behaves as a transcriptional activator of p53 (Alves da Costa et al., 2006). Here, we show that presenilins also control PrP^c transcription in a presenilin-dependent manner by increasing AICD-induced p53 expression. Our study is the first demonstration of the involvement of presenilins in the control of PrP^c expression and reveals a new pathway linking γ-secretase and p53 to the direct control of PrP^c transcription. Since endogenous PrP^c is necessary to allow $PrP^{s.c.}$ infectious process, presenilin-dependent control of PrP^c levels could be

Received Feb. 16, 2009; revised March 30, 2009; accepted April 17, 2009.

This work was supported by the Fondation pour la Recherche Médicale and by the Conseil Général des Alpes-Maritimes. We thank Drs. S. Pimplikar (Cleveland, OH), U. Müller (Heidelberg, Germany), M.F. Roussel (Memphis, TN), B. De Strooper (Leuven, Belgium), and P. Saftig (Göttingen, Germany) for kindly providing cell lines and brain samples. We sincerely thank T. C. Südhof (Dallas, TX), G. Thinakaran (Chicago, IL), J. C. Bourdon (Dundee, Scotland, UK), and L. Mercken (Vitry-sur-Seine, France) for their generous gift of cDNAs and antibodies.

Correspondence should be addressed to either Bruno Vincent or Frédéric Checler, Institut de Neuromédecine Moléculaire, UMR6097 CNRS/UNSA, 660 route des lucioles, 06560 Valbonne, France, E-mail: vincentb@ipmc.cnrs.fr or checler@ipmc.cnrs.fr.

DOI:10.1523/JNEUROSCI.0789-09.2009

 0270-6474/09/296752-09$15.00/0

seen as a means to modulate not only the physiological function of PrP^{c} but also $PrP^{s.c.}$ accumulation. This hypothesis is nicely supported by a recent study showing that a γ-secretase inhibitor significantly impairs the accumulation of pathogenic prions *in vivo* (Spilman et al., 2008), suggesting that such compounds could represent a new class of therapeutic agents against prion diseases.

Materials and Methods

Cell culture and transfections. Embryonic mouse fibroblasts [presenilin-deficient ($PS^{-/-}$), βAPP-deficient ($APP^{-/-}$), $APP^{-/-}/APLP2^{-/-}$, $p19^{Arf-/-}$, and $p19^{Arf-/-}/p53^{-/-}$, as well as their respective wild-type controls], βAPP-over-expressing HEK293 cells and primary cultured neurons were obtained and maintained in culture as previously described (Vincent et al., 1996; Kamijo et al., 1997; Marambaud et al., 1997; Heber et al., 2000; Herreman et al., 2000; Pardossi-Piquard et al. 2005). Transient transfections in HEK293 cells were performed with Lipofectamine 2000 reagent (Invitrogen), whereas fibroblasts were transiently transfected by means of the mouse embryonic fibroblasts Nucleofector kit (Amaxa Biosystems) as described previously (Sunyach et al., 2007).

Immunoprecipitation, SDS-PAGE, and Western blotting. N1-containing conditioned media were immunoprecipitated and submitted to 16.5% Tris-tricine gels as previously described (Vincent et al., 2000). βAPP, APLP1, APLP2, Fe65, Tip60, and p53 were separated on 8% Tris-glycine gels, whereas PrP^{c}, tubulin, PS1, and PS2 were analyzed on 12% Tris-glycine gels. C50 and C59 fragments were separated on 16.5% Tris-tricine gels. Proteins were then transferred onto Hybond-C nitrocellulose membranes and incubated with the following antibodies: monoclonal SAF32 (N1 and PrP^{c}; SPIBio), monoclonal anti-β-tubulin or anti-β-actin (Sigma), polyclonal anti-NTF-PS1 or anti-Loop-PS2 (Dr. Gopal Thinakaran, University of Chicago, Chicago, IL), polyclonal anti-Fe65 and monoclonal anti-myc (for myc-tagged C50 and C59; Dr. L. Mercken, Vitry-sur-Seine, France), monoclonal anti-HA (HA-tagged Tip60; Covance), polyclonal anti-APLP1 or APLP2 (EMD Biosciences), monoclonal 22C11 (βAPP; Roche Applied Science), or polyclonal anti-p53 (Dr. Jean-Christophe Bourdon, Dundee, Scotland, UK). Blots were revealed by incubations with goat anti-rabbit or goat anti-mouse secondary antibodies coupled to peroxidase (Beckman Coulter) and chemiluminescence recording using a Luminescence Image Analyzer LAS-3000 (Raytest). Quantification of data was performed with the Aida Image Analyzer software (Raytest).

Chronic γ-secretase inhibitor treatments. Chronic treatment of 4-d-old primary cultured neurons with the γ-secretase inhibitor DAPT (*N*-[-(3, 5-difluorophenacetyl)-L-alanyl]-*S*-phenylglycine t-butylester; 10 μM) was performed by addition of the inhibitor at 0 and 9 h for a total incubation of 24 h then PrP^{c} immunoreactivity was monitored by Western blot as described above.

Semiquantitative and real-time PCR analyses. Total RNA was extracted and purified from mouse embryonic fibroblasts or HEK293 cells with the NucleoSpin RNA II kit (Machery-Nagel). Two micrograms of total RNA were reverse-transcribed using oligo (dT) priming and avian myeloblastosis virus reverse transcriptase (Promega). For semiquantitative PCR, reactions were performed at 94°C for 30 s, then 55°C for 1 min, and finally 68°C for 2 min using 40 cycles, followed by a final extension of 7 min at 68°C. PCR products were analyzed on a 1% agarose gel stained with ethidium bromide. Real-time PCR were performed in an ABI PRISM 5700 sequence detector system (Applied Biosystems) using the SYBR Green detection protocol as outlined by the manufacturer. Specific primers for semiquantitative or real-time PCR were designed using the Primer Express software (Applied Biosystems) and were as follows: mouse PrP^{c}: forward, 5′-CTG CTG GCC CTC TTT GTG AC-3′ and reverse 5′-CTT TTT GCA GAG GCC GAC AT-3′. Human PrP^{c}: forward, 5′-AAT CAA GCA GCA CAC GGT CA-3′ and reverse 5′-TCG GTG AAG TTC TCC CCC TT-3′.

Expression levels of human p53 and PrP^{c} genes and mouse PrP^{c} gene were normalized by monitoring RNA levels of human GAPDH and mouse γ-actin genes using the following primers: forward, 5′-TGG GCT ACA CTG AGC ACC AG-3′ and reverse 5′-CAG CGT CAA AGG TGG AGG AG-3′ for human GAPDH; and forward 5′-CAC CAT CGG TTG TTA GTT GCC-3′ and reverse 5′-CAG GTG TCG ATG CAA ACG TT-3′ for mouse γ-actin.

Measurements of PrP^{c} promoter transactivation. The 1543 bp of the 5′ untranslated and promoter region of the human PrP^{c} gene was subcloned into the luciferase reporter vector pGL3basic and used to measure PrP^{c} promoter transactivation as has been extensively described (Funke-Kaiser et al., 2001). Cells grown in 12-well plates were cotransfected with PrP^{c} promoter-luciferase, β-galactosidase (to normalize transfection efficiencies), and the indicated cDNAs with Lipofectamine (HEK293 cells) or with the Amaxa Nucleofector kit (mouse embryonic fibroblasts). Thirty-six hours after transfection, luciferase and β-galactosidase activities were measured with appropriate enzyme assay systems (Promega).

Site-directed mutagenesis of PrP^{c} promoter. Mutation of the p53 putative binding site located on the human PrP^{c} promoter-luciferase reporter construct (Mahal et al., 2001) was introduced using the Quick change site-directed mutagenesis kit (Stratagene) following manufacturer's specifications. The two following sets of primers were purchased from Eurogentec: forward, 5′-CCTATTTTCCCCAGGGAGCACCTGGTTTACGCCC-3′; reverse, 5′-GGGCGTAAACCA-GGTGCTCCCTGGGGAAAATAGG-3′. The resulting construct (CATG replaced by AGCA) was verified by sequencing.

Chromatin immunoprecipitation assay. Chromatin immunoprecipitation assay (ChIP) was performed according to the instructions of the Chip-IT kit (Active Motif). Briefly, to prepare chromatin, HEK293 cells were seeded in three 150 mm dishes and allowed to reach 70–80% confluency. Cells were fixed, recovered in PBS, cross linked, and processed for chromatin preparation. DNA obtained was digested with the shearing enzyme provided in the kit as recommended by the supplier, yielding chromatin fragments of 200–500 bp in size. Each immunoprecipitation was performed on 50 μg of chromatin in the ChIP immunoprecipitation buffer supplied, with 5 μg of anti-p53 primary antibody (Active Motif) or irrelevant antibody (IgG and RNApol IgG) as negative controls. Immune complexes were collected with 40 μl of a solution of protein G-Sepharose. After elution, cross links were reversed and RNA digested using RNase (100 μg/ml). To digest proteins, SDS (1%), and proteinase K (100 μg/ml) were added, and the samples were incubated overnight at 37°C. The beads were washed as recommended and DNA was purified on columns provided. PCR amplification was performed using primers specific for the −326/−150 bp region of the PrP^{c} promoter (forward, 5′-CAGGAGCCACACAGTTGAAACAGA-3′; reverse, 5-AGGGTGATTTACGTAAAATAGCAAA-3′).

Transgenic mouse brain tissue preparation. Pieces of brains from $APP^{-/-}$ and $APP^{-/-}/APLP2^{-/-}$ mice (Heber et al., 2000), and Fe65 transgenic and Fe65/AICD transgenic mice (Ryan and Pimplikar, 2005), together with their respective wild-type controls, were homogenized in lysis buffer (10 mM Tris/HCl, pH 7.5, containing 150 mM NaCl, 0.5% Triton X-100, 0.5% deoxycholate, 5 mM EDTA). Protein expressions were analyzed by Western blot as described above.

Immunofluorescence analysis. Wild-type, $PS^{-/-}$, or $APP^{-/-}/APLP2^{-/-}$ fibroblasts were grown on glass coverslips in 35 mm dishes. At 50% of confluence, cells were fixed with 1.5% paraformaldehyde for 20 min at room temperature and washed three times with PBS. Permeabilization was performed by the addition of 0.1% Triton X-100 for 5 min followed by three PBS washes (nonpermeabilized cells were maintained in PBS during this time). After incubation for 1 h with 1% nonfat milk in PBS (to limit nonspecific fixation of antibodies), cells were incubated overnight at 4°C with the indicated primary antibodies in 1% nonfat milk/PBS). After three washes with PBS, cells were incubated for 1 h with adequate secondary antibodies conjugated to Alexa Fluor-594 and Alexa Fluor-488 respectively (Interchim). Coverslips were washed, incubated with DAPI to counterstain the nuclei and mounted in Vectashield-mounting medium (Vector Laboratories). Staining was visualized as previously described (Sunyach et al., 2007).

Statistical analysis. Statistical analyses were performed with the PRISM software (GraphPad) by using the unpaired *t* test for pairwise comparisons.

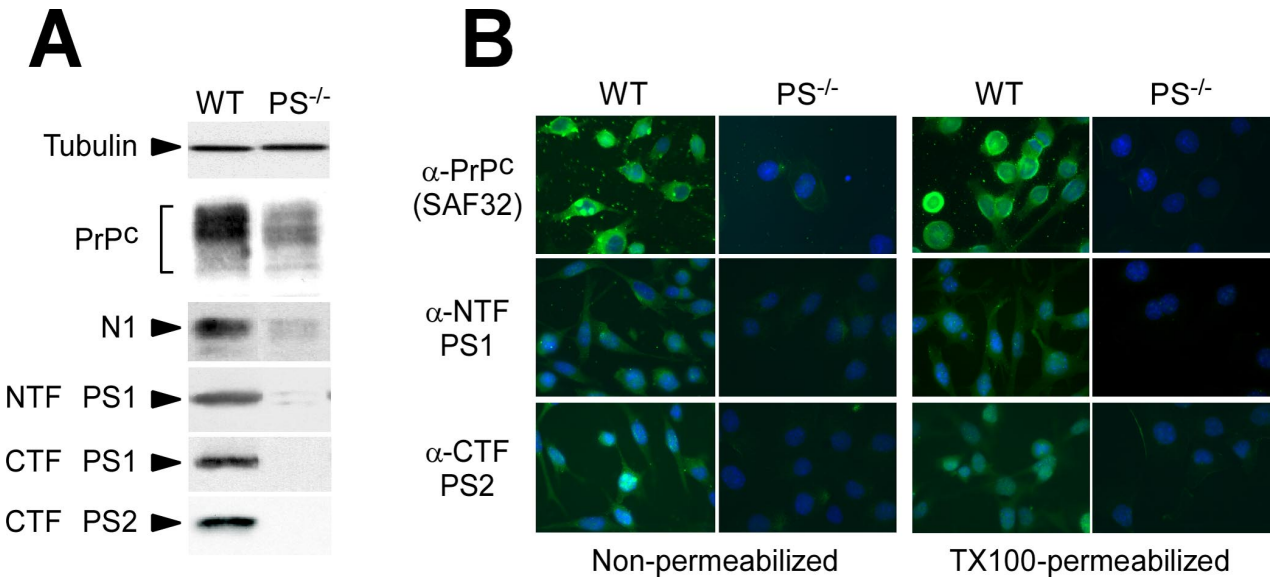

Figure 1. Presenilins deficiency reduces PrP^c immunoreactivity. ***A***, Wild-type (WT) or PS$^{-/-}$ mouse fibroblasts were incubated for 8 h in serum-free medium; then the secreted PrP^c N-terminal metabolite (N1) was immunoprecipitated and analyzed by 16.5% Tris/Tricine electrophoresis, and Western blot as described in Materials and Methods. PrP^c, tubulin, and presenilin 1 and 2 immunoreactivities were monitored in cell homogenates as described in Materials and Methods. ***B***, WT and PS$^{-/-}$ cells were fixed and labeled under nonpermeabilized or Triton X-100-permeabilized conditions with antibodies directed toward PrP^c (SAF32), N-terminal (NTF), and C-terminal (CTF) parts of presenilins (α-NTF PS1 and α-CTF PS2, respectively) as described in Materials and Methods. Cells were then counterstained with DAPI to visualize nuclei and analyzed on an Axioplan microscope.

Results

Presenilins modulate cellular prion protein at a transcriptional level

We examined the influence of presenilins on the expression of PrP^c. Figure 1*A* shows that PrP^c immunoreactivity was drastically decreased (50 ± 3.7% inhibition compared with wild-type cells, $n = 20$, $p < 0.0001$) in homogenates prepared from presenilins 1- and 2-deficient (PS$^{-/-}$) mouse fibroblasts. As expected, the secretion of the N-terminal metabolite of PrP^c referred to as N1 (Chen et al., 1995; Vincent et al., 2000, 2001) was concomitantly reduced by PS deficiency (Fig. 1*A*). *In situ* staining of PrP^c on nonpermeabilized intact cells revealed a drastic decrease in cell surface-associated immunofluorescence in PS-deficient fibroblasts (Fig. 1*B*, left panels). PrP^c labeling on Triton X-100 permeabilized cells revealed a similar decrease of PrP^c expression triggered by PS depletion (Fig. 1*B*, right panels), indicating that the reduction of membrane-associated PrP^c expression was not caused by an intracellular accumulation of the protein that would have been triggered by a defect in PS-dependent trafficking of PrP^c to the plasma membrane.

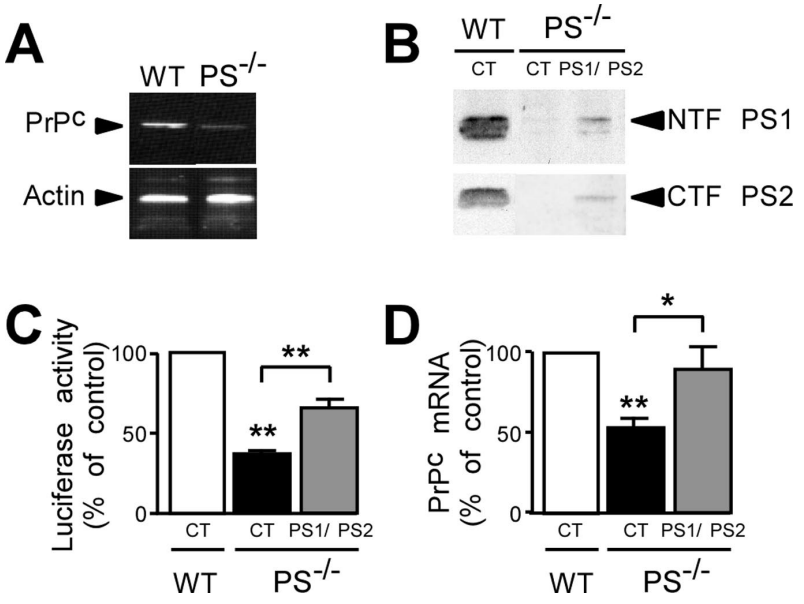

Figure 2. Presenilins regulate PrP^c expression at a transcriptional level. ***A***, Analysis of PrP^c and actin mRNA levels by semi-quantitative PCR in wild-type (WT) and PS$^{-/-}$ fibroblasts. ***B–D***, PS$^{-/-}$ fibroblasts were transiently transfected with either empty pcDNA3 vector (CT) or with PS1 and PS2 cDNA (PS1/PS2) as described in Materials and Methods. Thirty-six hours after transfection, protein expression (***B***), PrP^c promoter transactivation (***C***), and mRNA levels (***D***) were monitored. Bars in ***C*** and ***D*** express percentage of mock-transfected WT cells and represent the means ± SEM of 10 or 6 independent experiments, respectively. *$p < 0.05$; **$p < 0.0001$.

We assessed whether the observed reduction in PrP^c immunoreactivity resulted from a decrease in its mRNA transcription. We took advantage of the design of a PrP^c promoter construct that harbors 1543 bp of the 5′-untranslated promoter region of the PrP^c human gene in-frame with a luciferase reporter gene (Funke-Kaiser et al., 2001) to establish that PrP^c promoter transactivation was drastically reduced in PS-deficient fibroblasts (63 ± 2.5% of reduction compared with wild-type cells, $n = 15$, $p < 0.0001$) (Fig. 2*C*). This was accompanied by a lowering of PrP^c mRNA levels measured by both semiquantitative RT-PCR (Fig. 2*A*) and real-time PCR analyses (46.6 ± 8.4% of reduction, $n = 9$, $p < 0.0001$) (Fig. 2*D*) in PS-deficient fibroblasts. Importantly, we were able to substantially rescue PrP^c promoter transactivation (1.88 ± 0.13-fold increase, $p < 0.0001$) (Fig. 2*C*) and mRNA levels (1.69 ± 0.14-fold increase, $p < 0.05$) (Fig. 2*D*) after transient overexpression of both PS1 and PS2 in PS-deficient cells

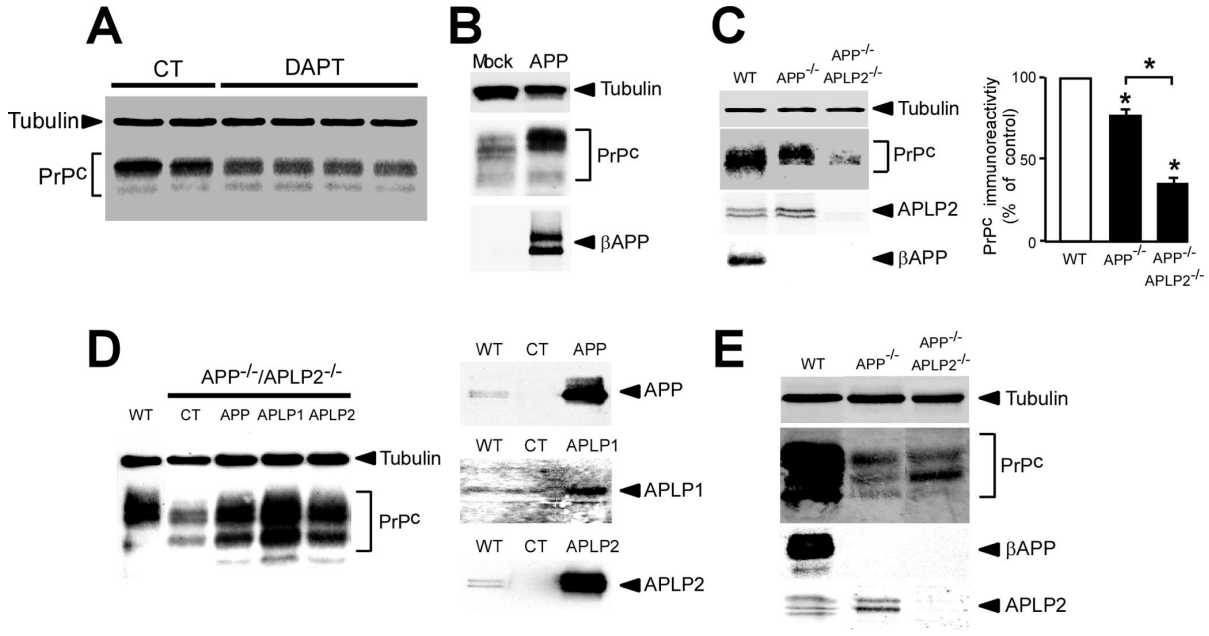

Figure 3. PrP^c expression is reduced by a γ-secretase inhibitor and is modulated by βAPP and APLP2 in cells and in mice brain. ***A***, Primary cultured neurons were chronically treated with the γ-secretase inhibitor DAPT (10 μM) for a total period of 24 h; then PrP^c and tubulin immunoreactivities were analyzed by Western blot as described in Materials and Methods. ***B***, PrP^c expression in stably transfected mock (mock)- and βAPP (APP)-expressing HEK293 cells (left). ***C***, PrP^c, tubulin, βAPP, and APLP2 immunoreactivities in homogenates of wild-type (WT), βAPP-deficient (APP$^{-/-}$), and APP$^{-/-}$/APLP2$^{-/-}$ fibroblasts (left) were monitored as described in Materials and Methods. Bars corresponding to densitometric analyses express percentage of control WT cells and represent the means ± SEM of 20 independent experiments. *$p < 0.0001$. ***D***, Empty pcDNA3 (CT), βAPP (APP), APLP1, or APLP2 cDNAs were transiently transfected in APP$^{-/-}$/APLP2$^{-/-}$ double knock-out fibroblasts. Thirty-six hours after transfection, PrP^c and tubulin immunoreactivities (left) or transgene expressions (right) were monitored as described in Materials and Methods. ***E***, PrP^c, tubulin, βAPP, and APLP2 immunoreactivities were monitored in whole homogenates prepared from WT, APP$^{-/-}$, and APP$^{-/-}$/APLP2$^{-/-}$ mice brains as described in Materials and Methods.

(Fig. 2*B*). Overall, the above data demonstrate that the PSs control PrP^c expression at the transcriptional level.

βAPP and APLPs are involved in the regulation of PrP^c transcription

PSs are pleiotropic proteins (Checler, 1999) that are thought to harbor an aspartyl protease activity referred to as γ-secretase (Wolfe et al., 1999). To assess whether the PS-dependent control of PrP^c expression could be linked to γ-secretase activity, primary cultured neurons were exposed to DAPT, a specific PS-directed inhibitor (Dovey et al., 2001). Figure 3*A* clearly shows that chronic treatment of neurons with DAPT significantly reduced PrP^c expression (37 ± 4% inhibition, $n = 3$, $p < 0.0001$). The βAPP is historically the first protein described as a substrate of the PS-dependent γ-secretase activity (De Strooper et al., 1998). Furthermore, PS-dependent cleavage of βAPP yields a C-terminal metabolite called AICD that has been suggested to behave as a transcription factor (Müller et al., 2008). We therefore examined whether βAPP could be involved in the control of PrP^c expression and promoter transactivation. We first showed that βAPP overexpression triggers a significant increase of PrP^c immunoreactivity (1.6 ± 0.07-fold increase, $n = 8$, $p < 0.0001$) (Fig. 3*B*) in human stably transfected HEK293. To rule out any artifactual effect resulting from overexpression procedure and to confirm that endogenous βAPP indeed controls PrP^c expression, we monitored PrP^c immunoreactivities in βAPP-deficient fibroblasts, and we observed a reduction of PrP^c expression in absence of βAPP (19.3 ± 3.6% inhibition, $p < 0.0001$) (Fig. 3*C*), a phenotype reminiscent of that observed in presenilin-deficient cells (Fig. 1*A*). Interestingly, the lowering of PrP^c expression was further amplified in βAPP$^{-/-}$/APLP2$^{-/-}$ fibroblasts (63 ± 6% inhibition, $p < 0.0001$) (Fig. 3*C*) that are lacking APLP2, a member of the βAPP family that also undergoes PS-dependent γ-secretase-like cleavages (Scheinfeld et al., 2002). Interestingly, we show that PrP^c immunoreactivity was fully restored by transient transfections of βAPP or APLP2 cDNAs in βAPP$^{-/-}$/APLP2$^{-/-}$ cells (Fig. 3*D*). It should be noted that APLP1, another member of the βAPP family that is expressed in the brain but absent in fibroblasts, mimics the potential of rescue harbored by βAPP and APLP2 (Fig. 3*D*). The above findings were further supported by *in vivo* data showing a dramatic reduction of PrP^c expression in both βAPP- and βAPP/APLP2-deficient mouse brains (Fig. 3*E*). Finally, immunofluorescence staining of PrP^c at the cell surface of permeabilized and nonpermeabilized βAPP$^{-/-}$/APLP2$^{-/-}$ cells indicated that the combined absence of βAPP and APLP2 drastically impaired PrP^c expression at the plasma membrane (Fig. 4*A*), as was observed in PS-deficient cells.

Four lines of data indicate that βAPP and APLP2 control PrP^c expression at a transcriptional level. First, the transactivation of the human PrP^c promoter was significantly impaired by βAPP and βAPP/APLP2 depletion (63 ± 5% reduction, $p < 0.0001$ and 81 ± 3% decrease, $p < 0.0001$, respectively) (Fig. 4*B*). Second, βAPP and βAPP/APLP2 deficiency lowered PrP^c mRNA levels as shown by semiquantitative (Fig. 4*C*) and quantitative real-time PCR (70 ± 14% decrease, $p < 0.01$ and 69 ± 10% inhibition, $p < 0.003$, respectively) (Fig. 4*D*). Third, βAPP partially restored both PrP^c promoter transactivation (2.07 ± 0.05-fold increase, $p < 0.0001$) and PrP^c mRNA levels (3.02 ± 0.37-fold increase, $p < 0.03$) (Fig. 4*E*). Fourth, both luciferase activity (2.75 ± 0.14-fold increase, $n = 6$, $p < 0.0001$) and PrP^c mRNA levels (1.93 ± 0.11-fold increase, $n = 10$, $p < 0.0001$) were significantly augmented after βAPP overexpression in HEK293 cells, ruling out a possible cell specific βAPP-mediated control of PrP^c transcription (data not shown).

The γ-secretase-derived βAPP metabolite AICD controls PrP^c expression and promoter transactivation

The βAPP-related effects on PrP^c expression and transcription were fully reminiscent of those associated with PSs. Since the latter appeared dependent on γ-secretase activity, we reasoned that the production of a βAPP metabolite generated by PS-dependent γ-secretase activity could account for the observed modulation of PrP^c mRNA levels and protein expression. Interestingly, AICD59 (C59) and AICD50 (C50) derive from the γ- and ε-secretase attacks of βAPP, respectively, and have been suggested to modulate a series of genes at a transcriptional level (Müller et al., 2008). Therefore, we examined the possibility that AICD could modulate the transcription of PrP^c. The adaptor protein Fe65 and the histone acetyltransferase Tip60 have been reported to enhance AICD immunoreactivity and to promote AICD translocation to the nucleus (Cao and Südhof, 2001). Therefore, we transiently transfected C50 or C59 together with Fe65 and Tip60 in βAPP$^{-/-}$/APLP2$^{-/-}$ fibroblasts (Fig. 5*A*). Clearly, both C50 and C59 overexpression significantly enhanced PrP^c immunoreactivity (1.14 ± 0.05-fold increase, $p < 0.005$ and 1.55 ± 0.16-fold increase, $p < 0.005$, respectively) (Fig. 5*A*), PrP^c promoter transactivation (1.13 ± 0.04-fold increase, $p < 0.002$ and 1.64 ± 0.12-fold increase, $p < 0.0001$, respectively) (Fig. 5*B*), and PrP^c mRNA levels (2.47 ± 0.12-fold increase, $p < 0.05$ and 1.73 ± 0.04-fold increase, $p < 0.05$, respectively) (Fig. 5*C*). Here again, both C50 and C59 heighten PrP^c mRNA levels (2.41 ± 0.26-fold increase, $p < 0.01$ and 1.68 ± 0.19-fold increase, $p < 0.03$, respectively) in HEK293 cells (Fig. 5*D*). Finally, we took advantage of transgenic mice overexpressing both C59 and Fe65 (Ryan and Pimplikar, 2005) to determine whether the AICD-mediated control of PrP^c expression described here also takes place *in vivo* in mouse brain. Indeed, C59/Fe65 transgenic mice show enhanced cerebral expression of PrP^c compared with Fe65 single transgenic animals (Fig. 5*E*). Since PS-dependent γ-secretase activity is able to cleave other substrates than βAPP, thereby generating other ICDs, we examined the effect of notch ICD (NICD), mΔENotch (which engenders NICD after γ-secretase cleavage), or the γ-secretase-derived C-terminal products of E- and N-cadherins (E-Cad/CTF2 and N-Cad/CTF2, respectively), and established that none of these fragments were able to modulate PrP^c levels (data not shown).

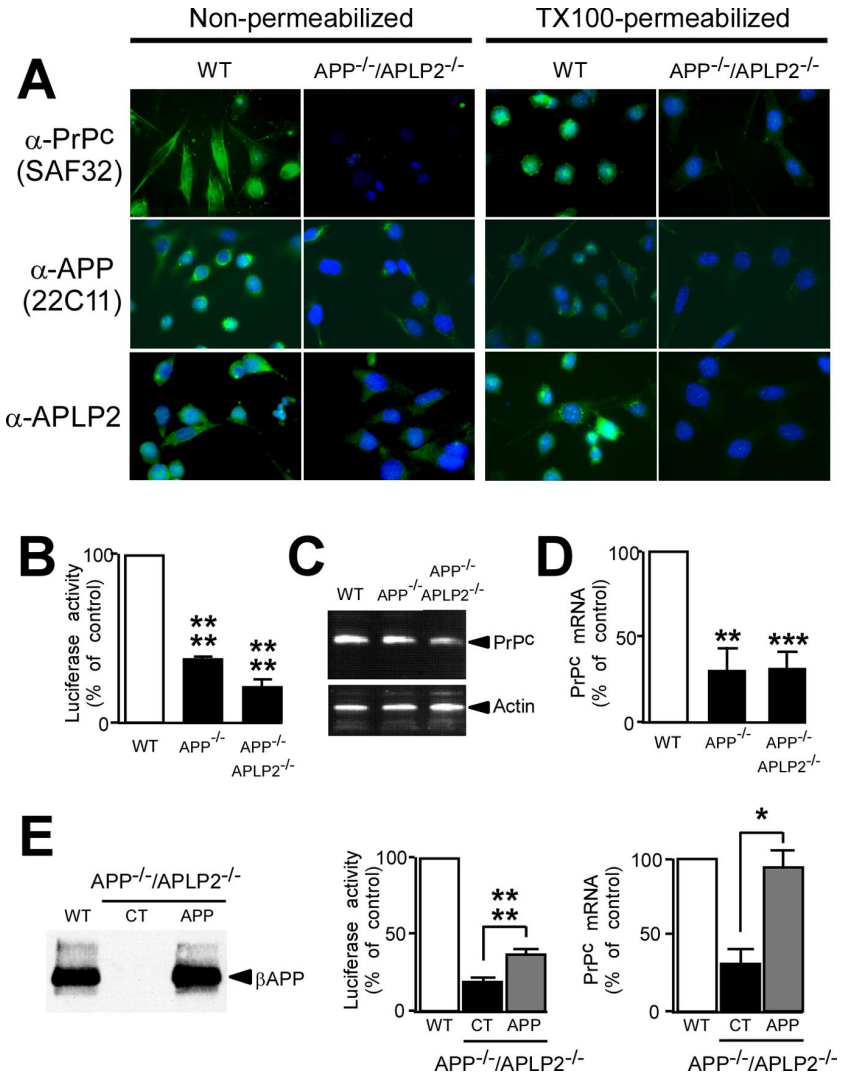

Figure 4. βAPP and APLP2 regulate PrP^c at a transcriptional level. ***A***, Wild-type (WT) and APP$^{-/-}$/APLP2$^{-/-}$ cultured fibroblasts were fixed and labeled with the indicated antibodies in nonpermeabilized or Triton X-100 permeabilized conditions as described in Materials and Methods. Cells were then counterstained with DAPI to visualize nuclei (in blue) and processed as described in Figure 1*B*. ***B***, Transactivation of the PrP^c promoter was measured in WT, APP$^{-/-}$, and APP$^{-/-}$/APLP2$^{-/-}$ cells as described in Materials and Methods. Bars corresponding to luciferase activities (normalized for β-galactosidase activities) express percentage of control activity recovered in WT cells and represent the means ± SEM of 20 independent experiments performed in triplicates. ****$p < 0.0001$. ***C***, ***D***, Analysis of PrP^c mRNA levels in WT, APP$^{-/-}$, and APP$^{-/-}$/APLP2$^{-/-}$ fibroblasts by semiquantitative (***C***) and real-time (***D***) PCR. Bars in ***D*** express percentage of control mRNA levels measured in WT cells and represent the means ± SEM of three independent experiments realized in triplicates. **$p < 0.01$; ***$p < 0.003$. ***E***, APP$^{-/-}$/APLP2$^{-/-}$ fibroblasts were transiently transfected with either empty pcDNA3 vector (CT) or βAPP cDNA. Thirty-six hours after transfection, βAPP immunoreactivity (left), PrP^c promoter transactivation (middle), and mRNA levels (right) were measured as described in Materials and Methods. Bars express percentage of control promoter transactivation or mRNA levels recovered in WT cells and represent the means ± SEM of 8 or 3 independent experiments, respectively. *$p < 0.03$; ****$p < 0.0001$.

AICD-mediated regulation of PrP^c is p53-dependent and occurs through direct binding of p53 to PrP^c promoter

The question arises by which mechanisms AICD could control PrP^c promoter transactivation, and thereby, mRNA and protein levels. We have previously demonstrated that AICDs can positively control p53 at the transcriptional level (Alves da Costa et al., 2006). *In silico* examination of the PrP^c promoter revealed a putative although incomplete p53-binding site (el-Deiry et al., 1992) (Fig. 6*B*). It was therefore tempting to speculate on the possibility that p53 could account for the AICD-mediated regulation of PrP^c transcription. Six lines of independent data confirm that this was indeed the case. First, PrPc mRNA levels were reduced by p53 depletion (Fig. 6*A*). Second, C50- and C59-mediated effects on PrP^c mRNA levels were fully p53-dependent because the C50/59-induced increase in PrP^c mRNA was prevented by p53 depletion (Fig. 6*A*). Third, PrP^c expression (de-

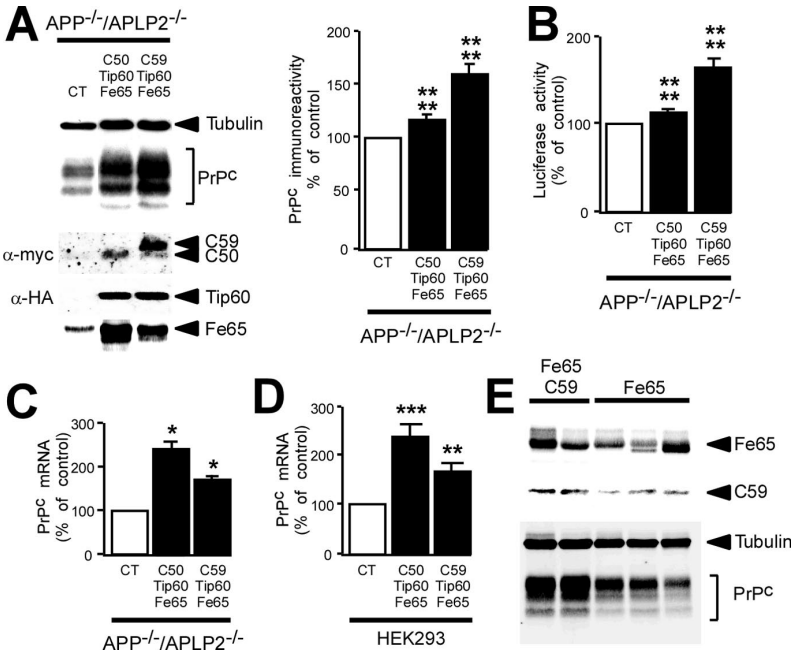

Figure 5. Presenilin-dependent control of PrP^c transcription is mediated by βAPP intracellular domains. ***A–C***, APP $^{-/-}$/APLP2 $^{-/-}$ fibroblasts were transiently transfected with empty pcDNA3 vector (CT) or C50/C59 cDNA together with Fe65 and Tip60-encoding plasmids as described in Materials and Methods. Thirty-six hours after transfection, PrP^c expression (***A***), promoter transactivation (***B***) and mRNA levels (***C***) were monitored as described in Materials and Methods. Bars express percentage of corresponding control values obtained with pcDNA3-transfected cells and represent the means ± SEM of 12 (***A***), 3 (***B***), or 4 (***C***) independent determinations. *$p < 0.05$; ****$p < 0.0003$. ***D***, HEK293 cells were transiently transfected with empty pcDNA3 vector (CT) or either C50 or C59 in combination with Fe65 and Tip60 cDNA in as described in Materials and Methods. Thirty-six hours after transfection, mRNA levels were monitored by real time PCR. Bars express percentage of control (pcDNA3-transfected cells) and represent the means ± SEM of 3 independent experiments performed in triplicates. **$p < 0.03$; ***$p < 0.01$. ***E***, Expressions of PrP^c, C59, Fe65, and tubulin were analyzed by Western blot, as described in Materials and Methods, in singly (Fe65) or doubly (Fe65/C59) transgenic mice brain homogenates.

crease of 34 ± 8%, $n = 5$, $p < 0.01$) (Fig. 6*C*), promoter transactivation (decrease of 49 ± 5%, $p < 0.001$) (Fig. 6*D*), and mRNA levels (decrease of 55 ± 15%, $p < 0.01$) (Fig. 6*E*) were reduced by p53 depletion. Fourth, p53 cDNA transfection in p53-deficient cells rescued PrP^c promoter activation (2.44 ± 0.07-fold increase, $p < 0.0001$) (Fig. 6*D*) and mRNA levels (2.6 ± 0.13-fold increase, $p < 0.001$) (Fig. 6*E*). Fifth, ChIP, using a set of primers framing the putative p53 binding site described above, showed that p53 physically bound to the human PrP^c promoter (Fig. 6*F*, lane 5). Sixth, mutation of the putative p53 binding site located on the PrP^c promoter reporter construct not only resulted in a significant decrease of baseline luciferase activity in p19$^{Arf\ -/-}$ cells expressing endogenous p53 levels (Fig. 6*G*, compare WT and Mut), but also abolished the ability of overexpressed p53 to trigger PrP^c promoter transactivation (Fig. 6*G*, compare WT/p53 and Mut/p53). This set of data brings the demonstration that p53 could act as a direct activator of PrP^c promoter transactivation and strongly argues in favor of a p53-mediated AICD-dependent regulation of PrP^c transcription.

Discussion

Although the role of the PrP^c in transmissible spongiform encephalopathies has been clearly established (Aguzzi and Polymenidou, 2004), its physiological function as well as the regulation of its expression are yet poorly understood. The demonstration that PrP^c-deficient mice are viable with no obvious deleterious phenotype (Büeler et al., 1992) would suggest either that endogenous PrP^c does not fulfill any vital functions, or that such functions could be complemented by yet unknown proteins/mechanisms. Nevertheless, several studies indicated that PrP^c could contribute to several distinct processes, including lymphocyte activation, synaptic transmission, cell adhesion, signaling, and apoptosis (for review, see Linden et al., 2008). Other works also suggested that PrP^c could be involved in the neuronal differentiation of PC12 cells triggered by either interleukin-6 or nerve growth factor, as shown by increased expression of PrP^c mRNA levels (Lazarini et al., 1994). Consistent with a pivotal link between NGF and PrP^c, PrP^c mRNA expression was also increased after intracerebral injection of this growth factor in cholinergic neurons (Mobley et al., 1988). Accordingly, Satoh et al. (1998) reported on cell-specific modulation of PrP^c mRNA levels after treatment with other cytokines (interleukin 1β), growth factors (tumor necrosis α), and tumor promoting drugs (phorbol esters).

Molecular cloning of the human *PRNP* gene promoter facilitated the understanding of the transcriptional regulation of PrP^c (Funke-Kaiser et al., 2001; Mahal et al., 2001). Thus, the 5′-flanking region of *PRNP* revealed several putative binding sites for transcription factors including Sp1, AP1, AP2, c-REL, and Nkx2–5, suggesting stimulus-dependent and cell-specific mechanisms of transcriptional regulation. Interestingly, Mahal et al. (2001) also reported a CATG sequence located 746 nt upstream to the transcriptional start site of the human *PRNP* gene. This CATG motif partially mimics the p53 consensus binding site sequence (el-Deiry et al., 1992). Whether this putative p53-binding domain was functional remained to be established. Nevertheless, the concomitant presence of p53 and SP-1 binding sequences on the *PRNP* promoter was interesting with respect to the fact that these two transcriptional factors were reported to physically interact to form functional hetero-complexes (Borellini and Glazer, 1993; MacLeod, 1993; Gualberto and Baldwin, 1995).

Our study clearly demonstrates that p53 acts as a functional activator of the *PRNP* gene promoter transcription. First, p53 deficiency drastically lowers PrP^c expression, mRNA levels, and promoter transactivation that all could be rescued by transient transfection of p53 cDNA. Second, substitution of the putative p53-binding site CATG by AGCA fully abolishes p53-dependent upregulation of PrP^c transcription. Third, ChIP unravels a direct interaction between p53 and PrP^c promoter. Therefore, our study establishes a physical and functional link between p53 and *PRNP* promoter triggering transcriptional activation and increased expression of PrP^c. Noteworthy, a very recent study described an ATM (ataxia-telangectasia-mutated)-mediated binding of p53 to the PRNP promoter in response to copper-induced oxidative stress that promotes an elevation of PrP^c (Qin et al., 2009).

It should be noted, however, that the *PRNP* gene did not emerge when a global mapping of p53-binding sites in the human

genome was performed recently by ChIP coupled to paired-end ditag sequencing (PET) (Wei et al., 2006). This likely reflects a weak physical *PRNP* promoter/p53 interaction as could have been expected from the fact that the human PrP^c promoter only contains one of the two canonical p53-binding CATG half-sites.

Since we previously established that PSs could modulate p53 expression (Alves da Costa et al., 2006), this prompted us to examine first whether PSs could control PrP^c expression. A first set of experiments clearly showed that PS depletion lowered PrP^c levels in cell homogenates as well as in intact cultured cells, and reduced PrP^c mRNA levels and its promoter transactivation. Interestingly, PrP^c immunoreactivity, promoter transactivation, and mRNA levels could be restored by PS1 and PS2 expression in PS-deficient fibroblasts. This clearly established that endogenous PSs could modulate PrP^c transcription. That this phenotype was linked to the reported ability of PSs to display γ-secretase activity was demonstrated by the fact that the presenilin-binding γ-secretase inhibitor DAPT indeed reduced PrP^c expression in primary cultured neurons.

PS-dependent γ-secretase targets a series of substrates (Wakabayashi and De Strooper, 2008) that could have been theoretically considered as putative mediators of p53-dependent PS-associated modulation of PrP^c. We examined the possibility that PS/γ-secretase-mediated cleavages of βAPP and APLP could be responsible for this phenotype, because we previously established that AICD and ALID (βAPP-like intracellular domain), the intracellular metabolites of the βAPP and APLP, respectively, generated by PS-dependent γ-secretase activity, could control p53 levels (Alves da Costa et al., 2006). Five lines of data indicate that this was indeed the case: first, βAPP overexpression increases PrP^c expression; second, βAPP and APLP depletion lowered PrP^c immunoreactivity, promoter transactivation. and mRNA levels in fibroblasts as well as in mice brains; third, βAPP and APLP cDNA transfection could rescue PrP^c promoter transactivation and mRNA levels in βAPP/APLP2 deficient cells; fourth, AICD increases PrP^c expression, promoter transactivation, and mRNA levels after overexpression in both βAPP/APLP2-deficient fibroblasts, whereas AICD-transgenic mice display higher PrP^c levels than wild-type animals; and fifth, AICD-mediated modulation of PrP^c mRNA levels was fully abolished by p53 deficiency. Overall, our study demonstrates for the first time that PSs control PrP^c levels via its ability to generate AICD. Thereafter, AICD increases p53 that ultimately acts as a transcriptional activator of *PRNP* gene promoter (Fig. 7). Moreover, it appears that AICD-mediated cascade leading to the modulation PrP^c is rather specific since other γ-secretase-derived fragments such as

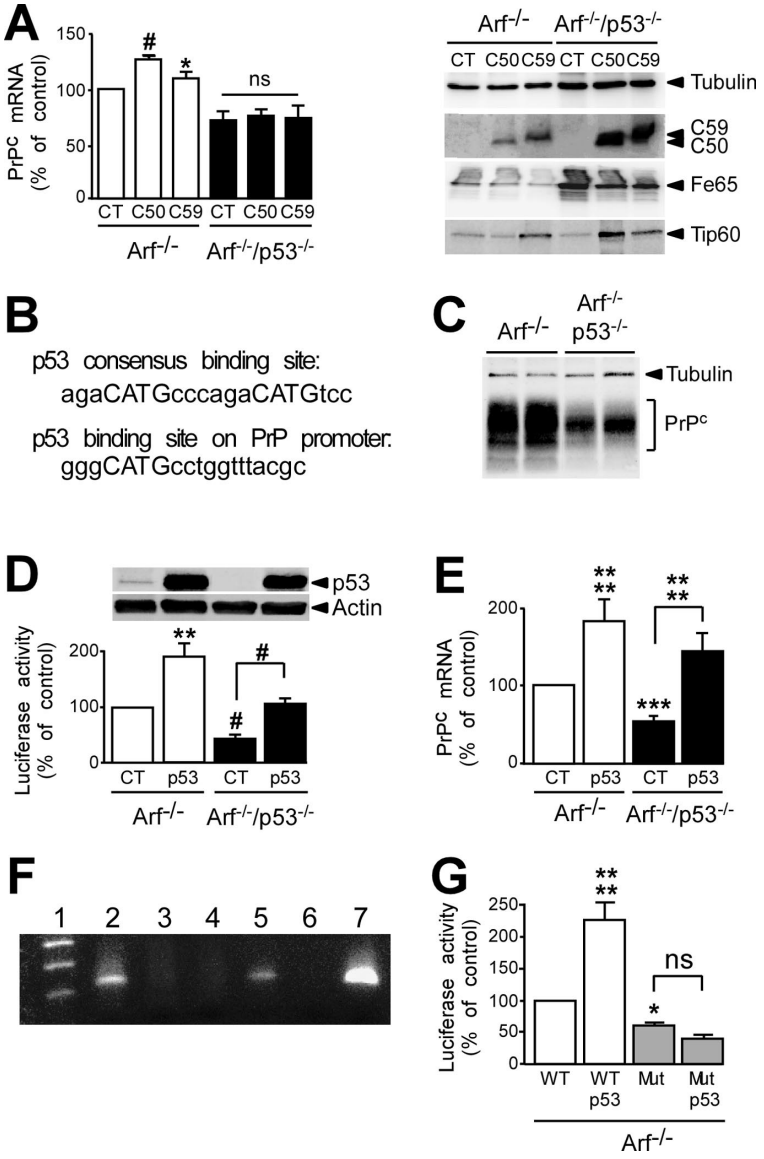

Figure 6. Regulation of PrP^c transcription by p53. ***A***, p19$^{Arf-/-}$ (Arf$^{-/-}$) and p19$^{Arf-/-}$p53$^{-/-}$ (Arf$^{-/-}$/p53$^{-/-}$) fibroblasts were transiently transfected with Fe65 and Tip60 cDNA together with either empty pcDNA3 vector (CT), C50 or C59 cDNA. Thirty-six hours after transfection, PrP^c mRNA levels were measured by real-time PCR as described in Materials and Methods. Right panel shows representative Western blot analyses of each of the over-expressed proteins. Bars express percentage of control (Arf$^{-/-}$ cells transfected with pcDNA3, Fe65 and Tip60 cDNA) and represent the means ± SEM of 4–8 experiments performed in duplicates. *$p < 0.05$; #$p < 0.0005$; ns, not statistically significant. ***B***, Alignment of typical p53 consensus binding motive (el-Deiry et al., 1992) with the partial p53-binding site identified on human PrP^c promoter (Mahal et al., 2001) where involved nucleotides are highlighted in high caps. ***C***, PrP^c expression was monitored in Arf$^{-/-}$ and Arf$^{-/-}$/p53$^{-/-}$ fibroblasts as described in Materials and Methods. ***D–E***, Arf$^{-/-}$ and Arf$^{-/-}$/p53$^{-/-}$ fibroblasts were transiently transfected with empty pcDNA3 vector (CT) or p53 cDNA. Thirty-six hours after transfection, PrP^c promoter transactivation (***D***) and RT-PCR analysis of mRNA levels (***E***) were monitored as described in Materials and Methods. Bars express percentage of control pcDNA3-transfected Arf$^{-/-}$ cells and represent the means ± SEM of 7 and 4 independent determinations, respectively. **$p < 0.01$; ***$p < 0.005$; ****$p < 0.001$; #$p < 0.0005$. ***F***, ChIP analysis of p53 binding on the PrP^c promoter sequence was performed as described in Materials and Methods. Lane 1: molecular markers, 2: DNA input, 3: IgG control, 4: RNA pol IgG, 5: anti p53 IgG, 6: water, 7: PrP^c promoter reporter construct. ***G***, Arf$^{-/-}$ fibroblasts were transiently transfected with pcDNA3 or p53 cDNA together with wild-type PrP^c promoter (WT, white bars) or with PrP^c promoter mutated on its partial p53-binding site (Mut, gray bars). Thirty-six hours after transfection, luciferase activity was measured as described in Materials and Methods. Values are expressed as a percentage of control (cells transfected with the wild-type PrP^c promoter alone, WT) and are the mean ± SEM of 6 experiments performed in triplicates. *$p < 0.05$; ****$p < 0.001$; ns, not significant.

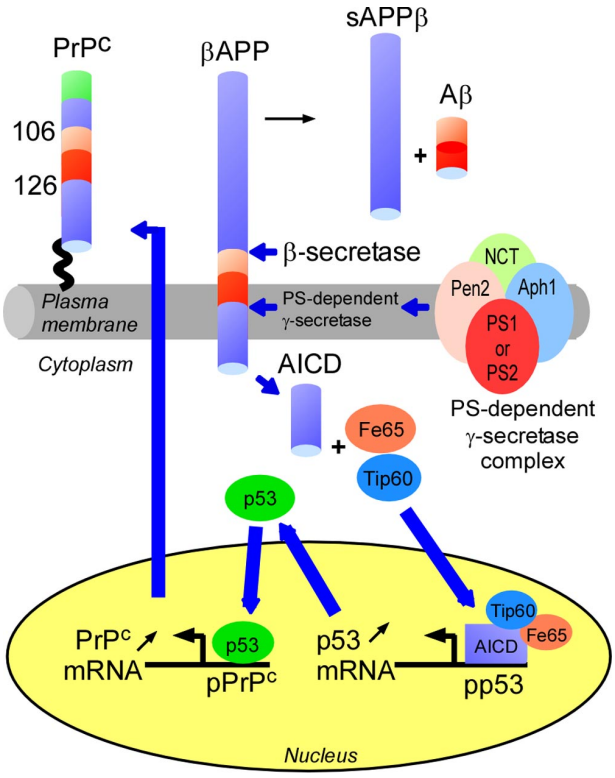

Figure 7. Schematic representation of the γ-secretase-mediated presenilin-dependent transcriptional activation of PrP^c via AICDs and p53. The cleavage of βAPP by the β-secretase BACE1 yields the C99 fragment that undergoes subsequent attack by the presenilin-dependent γ-secretase. This results in the concomitant productions of Aβ and AICD. AICD associates with the adaptor protein Fe65 and the histone acetyltransferase Tip60 to form a stable complex that translocates into the nucleus where it can induce the promoter transactivation of several gene targets including p53 (Alves da Costa et al., 2006) that acts as a direct activator of PrP^c promoter transactivation directly (this study). Therefore, PS-dependent γ-secretase-mediated production of AICD ultimately leads to a p53-dependent augmentation of cellular prion protein expression at the plasma membrane.

NICD or E- and N-cadherin C-terminal fragments did not affect PrP^c levels.

Interestingly, various neuropathological stigmata have previously been shown to label both Alzheimer's disease (AD)- and prion-affected brains (Powers et al. 1991; Hainfellner et al., 1998), and it has been reported that PrP^c gene polymorphism could increase the risk factor of developing early onset AD (Dermaut et al., 2003; Riemenschneider et al., 2004). Furthermore, cell biology approaches also indicated that several molecular effectors apparently bridge Alzheimer's disease and prion pathophysiology. Thus, PrP^c undergoes constitutive and PKC-regulated proteolysis by membrane-bound proteases of the disintegrin family of metalloproteases, namely ADAM10 and ADAM17 (Vincent et al., 2000, 2001). This proteolytic attack that takes place at the 111/112 peptidyl bond, i.e., in the middle of the putative neurotoxic 106–126 region of PrP^c (Forloni et al., 1993), is reminiscent of the well characterized α-secretase cleavage of βAPP, which occurs inside the Aβ sequence, is performed by the same enzymes, and is similarly upregulated by protein kinase C (Checler and Vincent, 2002). βAPP and PrP^c not only undergo common metabolic processes but can apparently cross talk. Thus, the levels of PrP^c and its distribution within cholesterol-rich lipid rafts strongly impact on the β-secretase cleavage of βAPP and thereby reduce Aβ production by restricting the access of BACE1 to βAPP (Parkin et al., 2007). Together with the present data, these observations establish that the secretases responsible for the metabolism of βAPP are also able to interfere with PrP^c physiology.

Several studies have clearly established that endogenous PrP^c was necessary for the PrP-scrapie-associated (PrP$^{s.c.}$) pathology since mice devoid of PrP^c resist infection by pathogenic inoculates (Büeler et al., 1993; Brandner et al., 1996). In this context, strategies aimed at reducing endogenous levels of PrP^c could be seen as theoretical methods to protect against prion infections. This could be envisioned by increasing disintegrin-mediated cleavages as we have proposed (Checler and Vincent, 2002). Is γ-secretase inhibition another putative therapeutic approach to interfere with prion propagation? This possibility has been supported by a recent very interesting study showing that an orally administered γ-secretase inhibitor, combined to quinacrine, was able to reduce PrP$^{s.c.}$ in the neocortex and hippocampus of mouse brains (Spilman et al., 2008). The present demonstration of a PS-dependent and γ-secretase-mediated control of PrP^c transcription provides the molecular basis of the above empirical observation and suggests that γ-secretase inhibitors could slow down the spread of pathogenic PrP$^{s.c.}$ in prion-infected animals simply by reducing its endogenous PrP^c template. Therefore, our work not only describes the tumor suppressor p53 as a transcriptional activator of *PRNP* gene promoter transcription but also unravels a new PS-dependent function in the control of PrP^c and potentially opens new perspectives concerning the treatment of prion-associated pathologies.

References

Aguzzi A, Polymenidou M (2004) Mammalian prion biology: one century of evolving concepts. Cell 116:313–327.

Alves da Costa C, Sunyach C, Pardossi-Piquard R, Sévalle J, Vincent B, Boyer N, Kawarai T, Girardot N, St George-Hyslop P, Checler F (2006) Presenilin-dependent γ-secretase-mediated control of p53-associated cell death in Alzheimer's disease. J Neurosci 26:6377–6385.

Bellingham SA, Coleman LA, Masters CL, Camakaris J, Hill AF (2009) Regulation of prion gene expression by transcription factors SP1 and MTF-1. J Biol Chem 284:1291–1301.

Borellini F, Glazer RI (1993) Induction of Sp1–p53 DNA-binding heterocomplexes during granulocyte/macrophage colony-stimulating factor-dependent proliferation in human erythroleukemiacell line TF-1. J Biol Chem 268:7923–7928.

Brandner S, Isenmann S, Raeber A, Fischer M, Sailer A, Kobayashi Y, Marino S, Weissmann C, Aguzzi A (1996) Normal host prion protein necessary for scrapie-induced neurotoxicity. Nature 379:339–343.

Büeler H, Fischer M, Lang Y, Bluethmann H, Lipp HP, DeArmond SJ, Prusiner SB, Aguet M, Weissmann C (1992) Normal development and behaviour of mice lacking the neuronal cell-surface PrP protein. Nature 356:577–582.

Büeler H, Aguzzi A, Sailer A, Greiner RA, Autenried P, Aguet M, Weissmann C (1993) Mice devoid of PrP are resistant to scrapie. Cell 73:1339–1347.

Cao X, Südhof TC (2001) A transcriptively active complex of APP with Fe65 and histone acetyltransferase Tip60. Science 293:115–120.

Cashman NR, Loertscher R, Nalbantoglu J, Shaw I, Kascsak RJ, Bolton DC, Bendheim PE (1990) Cellular isoform of the scrapie agent protein participates in lymphocyte activation. Cell 61:185–192.

Checler F (1999) Presenilins: multifunctional proteins involved in Alzheimer's disease pathology. IUBMB Life 48:33–39.

Checler F, Vincent B (2002) Alzheimer's and prion diseases: distinct pathologies, common proteolytic denominators. Trends Neurosci 25:616–620.

Chen SG, Teplow DB, Parchi P, Teller JK, Gambetti P, Autilio-Gambetti L (1995) Truncated forms of the human prion protein in normal brain and in prion diseases. J Biol Chem 270:19173–19180.

Dermaut B, Croes EA, Rademakers R, Van den Broeck M, Cruts M, Hofman A, van Duijn CM, Van Broeckhoven C (2003) PRNP Val129 homozygosity increases risk for early-onset Alzheimer's disease. Ann Neurol 53:409–412.

De Strooper B, Saftig P, Craessaerts K, Vanderstichele H, Guhde G, Von

Figura K, Van Leuven F (1998) Deficiency of presenilin 1 inhibits the normal cleavage of amyloid precursor protein. Nature 391:387–390.

Dovey HF, John V, Anderson JP, Chen LZ, de Saint Andrieu P, Fang LY, Freedman SB, Folmer B, Goldbach E, Holsztynska EJ, Hu KL, Johnson-Wood KL, Kennedy SL, Kholodenko D, Knops JE, Latimer LH, Lee M, Liao Z, Lieberburg IM, Motter RN, et al. (2001) Functional γ-secretase inhibitors reduce β-amyloid peptide levels in brain. J Neurochem 76:173–181.

el-Deiry WS, Kern SE, Pietenpol JA, Kinzler KW, Vogelstein B (1992) Definition of a consensus binding site for p53. Nat Genet 1:45–49.

Forloni G, Angeretti N, Chiesa R, Monzani E, Salmona M, Bugiani O, Tagliavini F (1993) Neurotoxicity of a prion protein fragment. Nature 362:543–546.

Funke-Kaiser H, Theis S, Behrouzi T, Thomas A, Scheuch K, Zollmann FS, Paterka M, Paul M, Orzechowski HD (2001) Functional characterization of the human prion protein promoter in neuronal and endothelial cells. J Mol Med 79:529–535.

Gauczynski S, Peyrin JM, Haïk S, Leucht C, Hundt C, Rieger R, Krasemann S, Deslys JP, Dormont D, Lasmézas CI, Weiss S (2001) The 37-kDa/67-kDa laminin receptor acts as the cell-surface receptor for the cellular prion protein. EMBO J 20:5863–5875.

Gualberto A, Baldwin AS Jr (1995) P53 and Sp1 interact and cooperate in the tumor necrosis factor-induced transcriptional activation of the HIV-1. J Biol Chem 270:19680–19683.

Hainfellner JA, Wanschitz J, Jellinger K, Liberski PP, Gullotta F, Budka H (1998) Coexistence of Alzheimer-type neuropathology in Creutzfeldt-Jakob disease. Acta Neuropathol 96:116–122.

Heber S, Herms J, Gajic V, Hainfellner J, Aguzzi A, Rülicke T, von Kretzschmar H, von Koch C, Sisodia S, Tremml P, Lipp HP, Wolfer DP, Müller U (2000) Mice with combined gene knock-outs reveal essential and partially redundant functions of amyloid precursor protein family members. J Neurosci 20:7951–7963.

Herreman A, Serneels L, Annaert W, Collen D, Schoonjans L, De Strooper B (2000) Total inactivation of γ-secretase activity in presenilin-deficient embryonic stem cells. Nat Cell Biol 2:461–462.

Kamijo T, Zindy F, Roussel MF, Quelle DE, Downing JR, Ashmun RA, Grosveld G, Sherr CJ (1997) Tumor suppression at the mouse INK4a locus mediated by the alternative reading frame product $p19^{ARF}$. Cell 91:649–659.

Kanaani J, Prusiner SB, Diacovo J, Baekkeskov S, Legname G (2005) Recombinant prion protein induces rapid polarization and development of synapses in embryonic rat hippocampal neurons *in vitro*. J Neurochem 95:1373–1386.

Lazarini F, Castelnau P, Chermann JF, Deslys JP, Dormont D (1994) Modulation of prion protein expression by growth factors in cultured mouse astrocytes and PC-12 cells. Mol Brain Res 22:268–274.

Linden R, Martins VR, Prado MA, Cammarota M, Izquierdo I, Brentani RR (2008) Physiology of the prion protein. Physiol Rev 88:673–728.

MacLeod MC (1993) Identification of a DNA structural motif that includes the binding sites for Sp1, p53 and GA-binding protein. Nucleic Acids Res 21:1439–1447.

Mahal SP, Asante EA, Antoniou M, Collinge J (2001) Isolation and functional characterization of the promoter region of the human prion protein gene. Gene 268:105–114.

Mangé A, Milhavet O, Umlauf D, Harris D, Lehmann S (2002) PrP-dependent cell adhesion in N2a neuroblastoma cells. FEBS Lett 514:159–162.

Marambaud P, Chevallier N, Barelli H, Wilk S, Checler F (1997) Proteasome contributes to the α-secretase pathway of amyloid precursor protein in human cells. J Neurochem 68:698–703.

Mobley WC, Neve RL, Prusiner SB, McKinley MP (1988) Nerve growth factor increases mRNA levels for the prion protein and the β-amyloid protein precursor in developing hamster brain. Proc Natl Acad Sci U S A 85:9811–9815.

Mouillet-Richard S, Ermonval M, Chebassier C, Laplanche JL, Lehmann S, Launay JM, Kellermann O (2000) Signal transduction through prion protein. Science 289:1925–1928.

Müller T, Meyer HE, Egensperger R, Marcus K (2008) The amyloid precursor protein intracellular domain (AICD) as modulator of gene expression, apoptosis, and cytoskeletal dynamics – relevance for Alzheimer's disease. Prog Neurobiol 85:393–406.

Pardossi-Piquard R, Petit A, Kawarai T, Sunyach C, Alves da Costa C, Vincent B, Ring S, D'Adamio L, Shen J, Müller U, St Georges-Hyslop P, Checler F (2005) Presenilin-dependent transcriptional control of the Aβ-degrading enzyme neprilysin by intracellular domains of βAPP and APLP. Neuron 46:541–554.

Parkin ET, Watt NT, Hussain I, Eckman EA, Eckman CB, Manson JC, Baybutt HN, Turner AJ, Hooper NM (2007) Cellular prion protein regulates β-secretase cleavage of the Alzheimer's amyloid precursor protein. Proc Natl Acad Sci U S A 104:11062–11067.

Powers JM, Liu Y, Hair LS, Kascsack RJ, Lewis LD, Levy LA (1991) Concomitant Creutzfeldt-Jakob and Alzheimer's disease. Acta Neuropathol 83:95–98.

Prusiner SB (1998) Prions. Proc Natl Acad Sci U S A 95:13363–13383.

Qin K, Zhao L, Ash RD, McDonough WF, Zhao RY (2009) ATM-mediatedtranscriptional elevation of prion in response to copper-induced oxidative stress. J Biol Chem 284:4582–4593.

Rieger R, Edenhofer F, Lasmézas CI, Weiss S (1997) The human 37-kDa laminin receptor precursor interacts with the prion protein in eucaryotic cells. Nat Med 3:1383–1388.

Riemenschneider M, Klopp N, Xiang W, Wagenpfeil S, Vollmert C, Müller U, Förstl H, Illig T, Kretzschmar H, Kurz A (2004) Prion protein codon 129 polymorphism and risk of Alzheimer disease. Neurology 63:364–366.

Ryan KA, Pimplikar SW (2005) Activation of GSK-3 and phosphorylation of CRMP2 in transgenic mice expressing APP intracellular domain. J Cell Biol 171:327–335.

Santuccione A, Sytnyk V, Leshchyns'ka I, Schachner M (2005) Prion protein recruits its neuronal receptor NCAM to lipid rafts to activate P59fyn and to enhance neurite outgrowth. J Cell Biol 169:341–354.

Satoh J, Kurohara K, Yukitake M, Kuroda Y (1998) Constitutive and cytokine-inducible expression of prion protein gene in human neuronal cell lines. J Neuropathol Exp Neurol 57:131–139.

Scheinfeld MH, Ghersi E, Laky K, Fowlkes BJ, D'Adamio L (2002) Processing of β-amyloid precursor-like protein-1 and -2 by γ-secretase regulates transcription. J Biol Chem 277:44195–44201.

Spilman P, Lessard P, Sattavat M, Bush C, Tousseyn T, Huang EJ, Giles K, Golde T, Das P, Fauq A, Prusiner SB, Dearmond SJ (2008) A γ-secretase inhibitor and quinacrine reduce prions and prevent dendritic degeneration in murine brains. Proc Natl Acad Sci U S A 105:10595–10600.

Sunyach C, Cissé MA, da Costa CA, Vincent B, Checler F (2007) The C-terminal products of cellular prion protein processing, C1 and C2, exert distinct influence on p53-dependent staurosporine-induced caspase-3 activation. J Biol Chem 282:1956–1963.

Vincent B, Beaudet A, Dauch P, Vincent JP, Checler F (1996) Distinct properties of neuronal and astrocytic endopeptidase 3.4.24.16: a study on differenciation, subcellular distribution and secretion processes. J Neurosci 16:5049–5059.

Vincent B, Paitel E, Frobert Y, Lehmann S, Grassi J, Checler F (2000) Phorbol ester-regulated cleavage of normal prion protein in HEK293 human cells and murine neurons. J Biol Chem 275:35612–35616.

Vincent B, Paitel E, Saftig P, Frobert Y, Hartmann D, De Strooper B, Grassi J, Lopez-Perez E, Checler F (2001) The disintegrins ADAM10 and TACE contribute to the constitutive and phorbol-esters-regulated normal cleavage of the cellular prion protein. J Biol Chem 276:37743–37746.

Wakabayashi T, De Strooper B (2008) Presenilins: members of the gamma-secretase quartets, but part-time soloists too. Physiology 23:194–204.

Wei CL, Wu Q, Vega VB, Chiu KP, Ng P, Zhang T, Shahab A, Yong HC, Fu Y, Weng Z, Liu J, Zhao XD, Chew JL, Lee YL, Kuznetsov VA, Sung WK, Miller LD, Lim B, Liu ET, Yu Q, Ng HH, Ruan Y (2006) A global map of p53 transcription-factor binding sites in the human genome. Cell 124:207–219.

Wolfe MS, Xia W, Ostaszewski BL, Diehl TA, Kimberly WT, Selkoe DJ (1999) Two transmembrane aspartates in presenilin-1 required for presenilin endoproteolysis and γ-secretase activity. Nature 398:513–517.